

Supporting Information

Nonsense-mediated decay regulates key components of homologous recombination

Ryan Janke^{1*}, Jeremy Kong¹, Hannes Braberg², Greg Cantin³, John R. Yates III³, Nevan J. Krogan^{2, 4, 5} and Wolf-Dietrich Heyer^{1,6}

¹ Department of Microbiology and Molecular Genetics, University of California, Davis, CA 95616-8665, USA

² Department of Cellular and Molecular Pharmacology, University of California, San Francisco, San Francisco, CA 94158-2517, USA

³ Department of Cell Biology, SR-11, Scripps Research institute, La Jolla, CA 92307

⁴ California Institute for Quantitative Biosciences, QB3, San Francisco, CA 94158-2517, USA

⁵ J. David Gladstone Institute, San Francisco, CA 94158-2517, USA

⁶ Department of Molecular and Cellular Biology University of California, Davis, CA 95616-8665, USA

*To whom the correspondence should be addressed: Tel. 530-752-3001; Fax 530-752-3011;
Email wdheyer@ucdavis.edu

Present address: [Ryan Janke] Department of Molecular and Cell Biology, California Institute for Quantitative Biosciences, QB3, University of California, Berkeley, Berkeley, California 94720-3220, USA

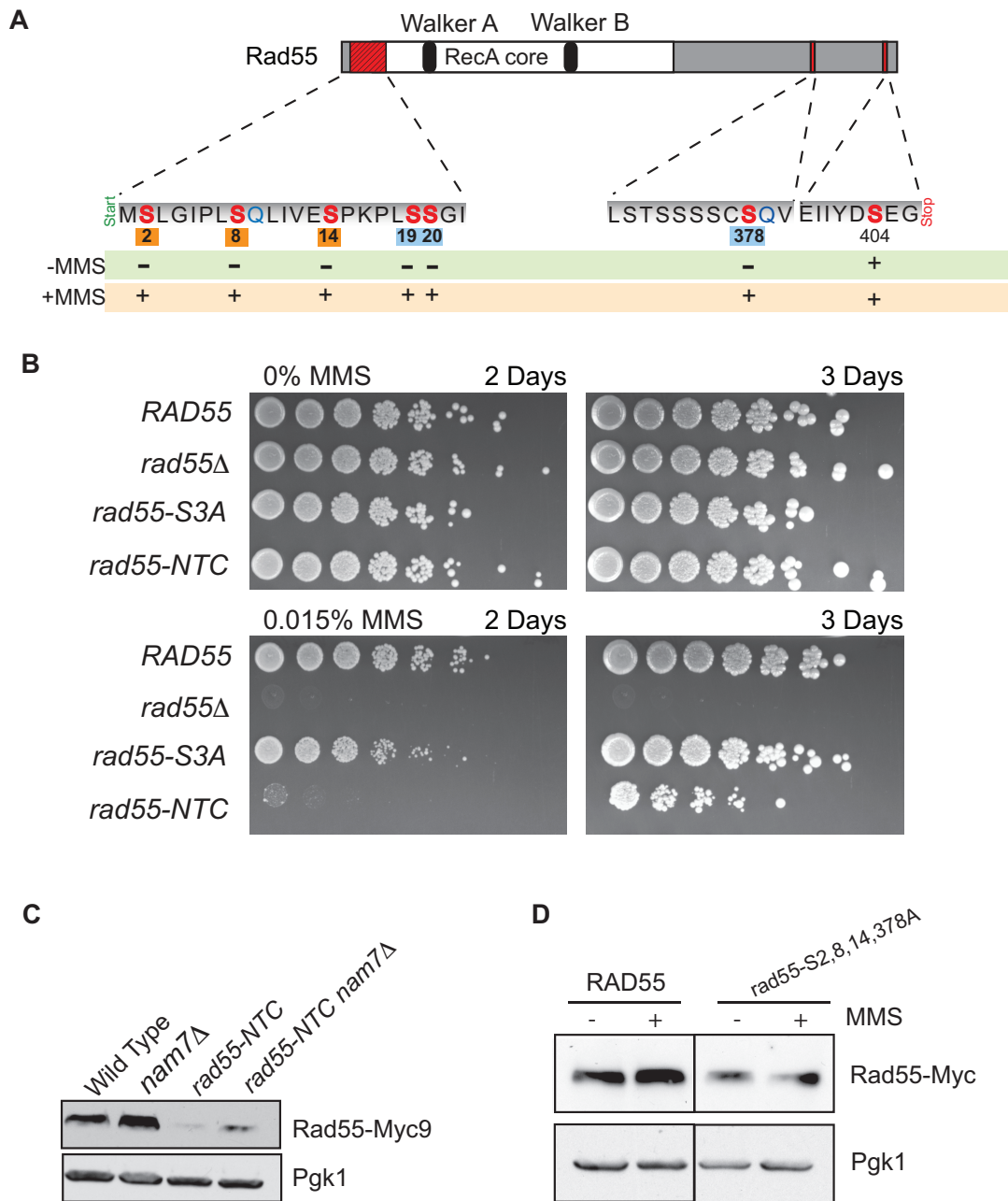


Figure S1. Characterization of Rad55 phosphorylation sites S19 and S20.

(A) Schematic of Rad55 phosphorylation sites mapped to their location on the Rad55 protein. Status of each phosphorylation site in -MMS and +MMS samples are indicated. Bold font of phosphorylation sites indicates those utilized in this study, while color indicates a role in protein function (orange) or stability (blue). (B) Plate assay testing the sensitivity of wild type, *rad55-Δ*,

rad55-S2, 8, 14A (abbreviated as *rad55-S3A*), and *rad55-S2,8,14,19,20A* (abbreviated as *rad55-NTC*) to MMS. (C) Immunoblots on Myc9-tagged Rad55 and Rad55-S2,8,14,19,20A (abbreviated as *rad55-NTC*) from cells with or without functioning NMD. The same membranes were reprobbed for Pgk1 to serve as a loading control. (D) Immunoblots of 9Myc-tagged Rad55 or Rad55-S2,8,14,378A from untreated cells or cells treated with 0.075% MMS for 1 hour. The same membranes were reprobbed with Pgk1 to serve as a loading control. In order to aid in visual comparison and exclude irrelevant intermediary lanes, the images were spliced from a single gel as indicated by the vertical bar separating Rad55 from Rad55-S2,8,14,378A. The 9myc and Pgk1 images were each obtained from a single scan of the same membrane.

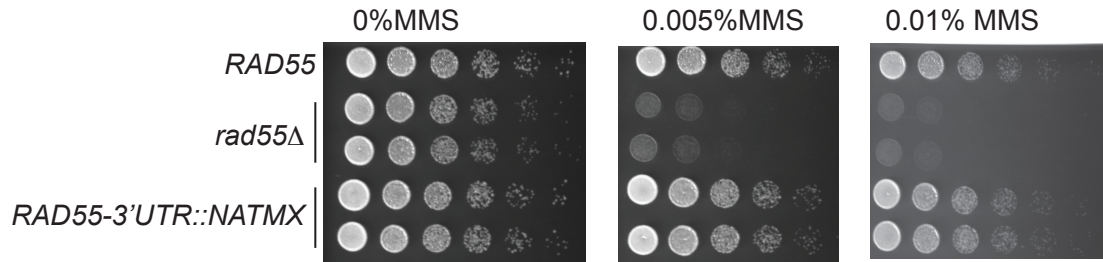


Figure S2. A *natMX* marker in the 3'-UTR of *RAD55* does not interfere with normal Rad55 function in E-MAP query strains.

A *natMX* marker was integrated 25 bp downstream from the *RAD55* stop codon to allow for selection of *rad55* point mutants in E-MAP analysis. Plate assays were performed on the E-MAP query strain containing this marker to ensure it did not lead to increased sensitivity to MMS. Lack of sensitivity indicates this marker does not have adverse effects on normal Rad55 function.

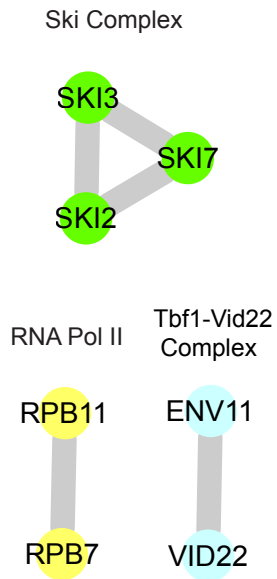


Figure S3. Additional pathways identified in E-MAP. A network of previously curated physical protein interactions was generated using GeneMANIA for positively interacting array genes identified applying the criteria used for Figure 1A.

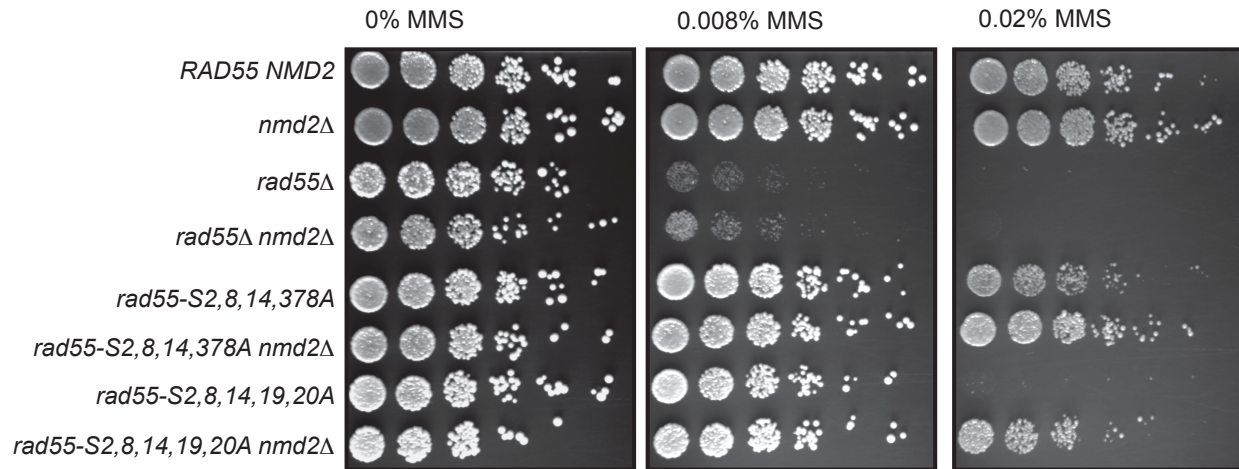


Figure S4. *rad55* phosphorylation site mutants are suppressed by *nmd2Δ*.

Plate assays were performed with W303 strains containing the indicated mutations. YPD plates containing 0% MMS, 0.008% MMS, or 0.02% MMS were incubated at 30° C for two days prior to imaging.

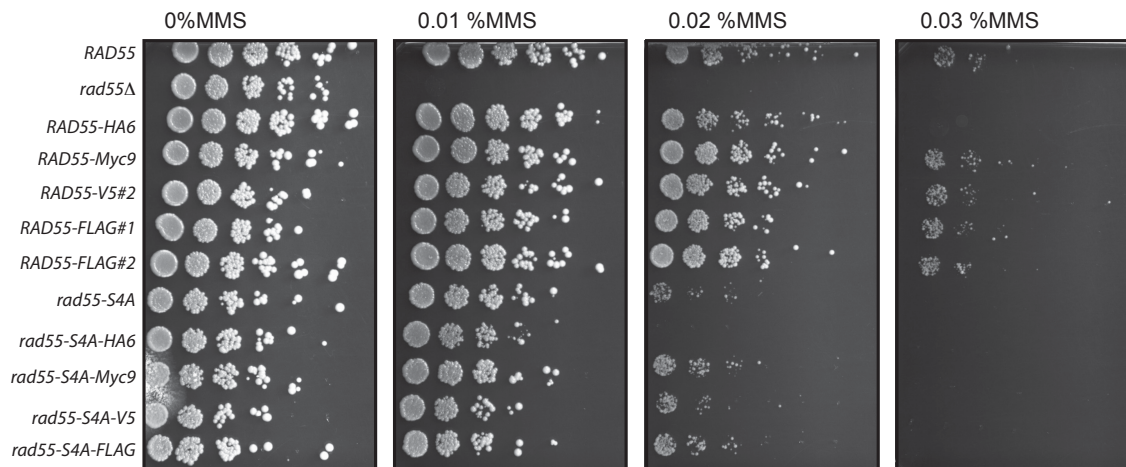


Figure S5. Plate assay of epitope tagged Rad55 strains

The indicated strains were tested across various concentrations of MMS to determine whether C-terminal epitope tagging of Rad55 interferes with Rad55 function. 5-fold serial dilutions of cultures were plated and grown at 30° C for 3 days prior to imaging plates. Genotype *rad55-S2, 8, 14, 378A* is abbreviated as *rad55-S4A*.

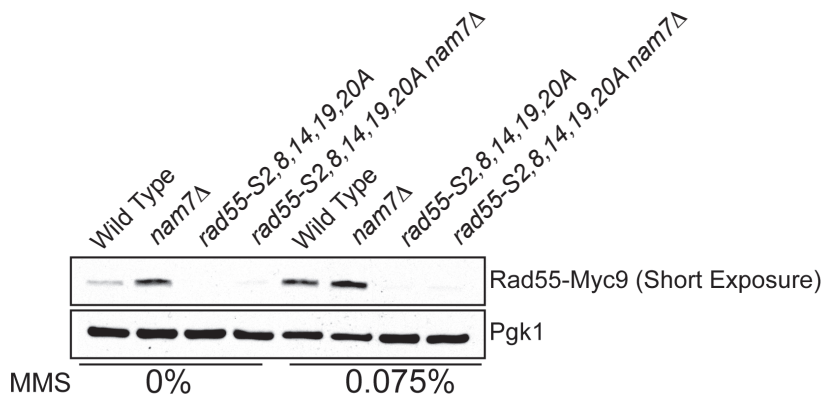


Figure S6. Representative exposure used to quantify wild type Rad55 levels by densitometry.

The large difference in steady state levels of Rad55 and Rad55-S2,8,14,19,20A precluded the possibility to obtain a single immunoblot exposure in which all Rad55 samples were within the linear range required for quantitative densitometry. Therefore wild type Rad55 and Rad55-S2,8,14,19,20A signals were quantified from separate short and long exposures. A short exposure used to quantify wild type Rad55 levels is shown here. A long exposure is shown in Figure 4A from which Rad55-S2,8,14,19,20A levels were quantified.

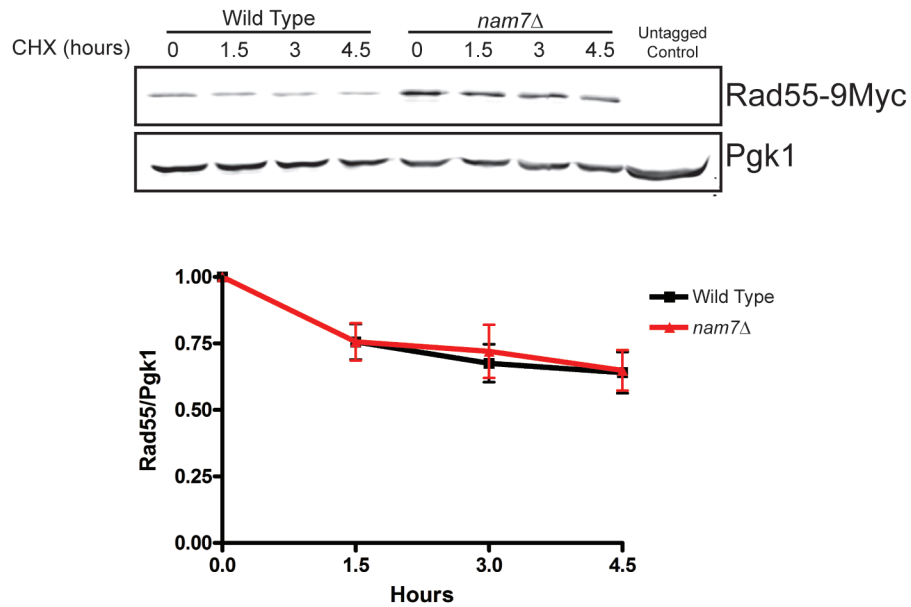
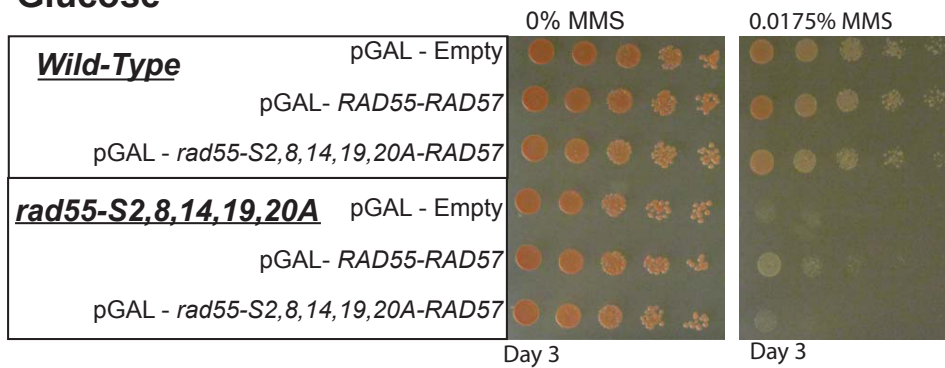


Figure S7. Cycloheximide chase measurement of Rad55 protein turnover

Rad55 protein turnover was assessed in wild type and *nam7Δ* strains by spiking cultures with 200 $\mu\text{g/ml}$ of cycloheximide and harvesting cells over the indicated time points. Rad55 levels were determined by immunoblotting for the C-terminal 9myc tag on Rad55 (upper panel). A control strain lacking the myc tag on Rad55 is labeled as ‘untagged control’. Immunoblot signals were quantified (lower panel). For each time point, the Rad55 signal was normalized to the Pgk1 signal and the fold change from the “0 hour” time point was plotted. Each point represents an average determined from three independent replicates. Error bars show standard error of the mean.

Glucose



Galactose

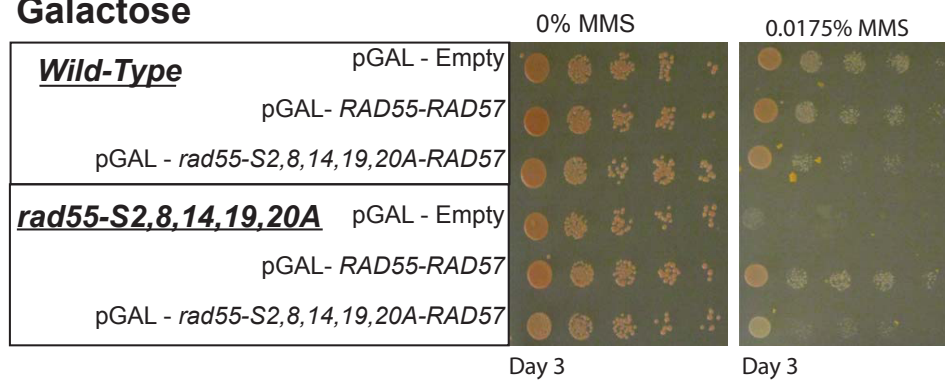


Figure S8. Overexpression of Rad55-S2,8,14,19,20A suppresses the MMS sensitivity of this mutant.

Plate assay testing the MMS sensitivity of wild type and *rad55-S2,8,14,19,20A* mutant strains when either wild type Rad55 or Rad55-S2,8,14,19,20A is overexpressed. Strains were transformed with a previously described galactose-inducible dual promoter expression plasmid (1) This plasmid contains both *RAD55* (or *rad55-S2,8,14,19,20A*) and *RAD57* under the gal1-10 bidirectional promoter. Cells grown in the presences of galactose express both Rad55 and Rad57 to maintain equal 1:1 stoichiometry. Cells were grown on SD-URA to maintain the plasmid. Overnight cultures were grown in CSM-URA with either 2% glucose or galactose overnight, diluted, and spotted onto SD-URA containing the same sugar and the indicated amount of MMS.

Supplemental Reference

1. Bashkirov, V.I., Herzberg, K., Haghazari, E., Vlasenko, A.S. and Heyer, W.D. (2006) DNA-damage induced phosphorylation of Rad55 protein as a sentinel for DNA damage checkpoint activation in *S. cerevisiae*. *Meth. Enzymol.*, **409**, 166-182.

Table S1. EMAP query strains used in this study.

Strain	Relevant Genotype
WDHY2832	Wild Type EMAP Query Strain
WDHY2898	<i>rad55-Δ::natMX</i>
WDHY2899	<i>RAD55- 3'UTR::natMX</i>
WDHY2952	<i>rad55-S2,8,14A-3'UTR::natMX</i>
WDHY2975	<i>rad55-S2,8,14,19,20A-3'UTR::natMX</i>
WDHY3069	<i>rad55-S378D-3'UTR::natMX</i>
WDHY3070	<i>rad55-S378A-3'UTR::natMX</i>
WDHY3072	<i>rad55-S2,8,14D-3'UTR::natMX</i>
WDHY3074	<i>rad55-S2,8,14,378A-3'UTR::natMX</i>

Strains contain the common genotype *MATα his3Δ1 leu2Δ0 ura3Δ0 met15Δ0 LYS2+ can1Δ::MATαPr-HIS3 lyp1Δ::MATαPr-LEU2*

Table S2. S-cores for RAD55 E-MAP interaction Screen

Separate Excel Spreadsheet file.

Table S3. *S. cerevisiae* strains used in this study.

Strain	Relevant Genotype
WDHY2009	<i>rad55-Δ::URA3(K. lactis)</i>
WDHY2217	<i>ura3-Δ::loxP</i>
WDHY2371	<i>can1-100 his3-11,15 leu2-3,112 trp1-1 ura3-1 RAD5 ade2-n-URA3-ade2-a</i>
WDHY2569	<i>ura3-Δ::loxP rad55-S2,8,14,19,20A</i>
WDHY2945	<i>rad55-S2,8,14,378A</i>
WDHY2972	<i>ura3-Δ::loxP RAD55-Myc9::TRP1(K. lactis)</i>
WDHY3449	<i>ura3-Δ::loxP rad55-S2,8,14,19,20A-Myc9::TRP1(K. lactis)</i>
WDHY3865	<i>ura3::LoxP nam7-Δ::natMX</i>
WDHY3866	<i>rad55-Δ::URA3(K. lactis) nam7-Δ::natMX</i>
WDHY3867	<i>ura3::LoxP nam7-Δ::natMX rad55-S2,8,14,19,20A</i>
WDHY3980	<i>ura3::LoxP rad55-S2,8,14,19,20A-Myc9::TRP1(K. lactis) nam7-Δ::natMX</i>
WDHY3982	<i>ura3::LoxP RAD55-Myc9::TRP1(K. lactis) nam7-Δ::natMX</i>
WDHY3984	<i>nam7-Δ::natMX rad55-S2,8,14,19,20A rad51-Δ::hisMX</i>
WDHY3890	<i>nam7-Δ::natMX rad51-Δ::hisMX</i>
WDHY3897	<i>rad51-Δ::hisMX</i>
WDHY4012	<i>nmd2-Δ::natMX</i>
WDHY4013	<i>nmd2-Δ::natMX rad55-Δ::URA3(K. lactis)</i>
WDHY4014	<i>nmd2-Δ::natMX rad55-S2,8,14,378A</i>
WDHY4015	<i>nmd2-Δ::natMX rad55-S2,8,14,19,20A</i>
WDHY4057	<i>ade2-1 can1-100 his3-11,15 leu2-3,112 trp1-1 rpb1-1</i>
WDHY4103	<i>ade2-1 can1-100 his3-11,15 leu2-3,112 trp1-1 rpb1-1 nam7-Δ::natMX</i>
WDHY4650	<i>can1-100 his3-11,15 leu2-3,112 trp1-1 ura3-1 RAD5 ade2-n-URA3-ade2-a</i> <i>nmd2-Δ::natMX</i>
WDHY4660	<i>can1-100 his3-11,15 leu2-3,112 trp1-1 ura3-1 RAD5 ade2-n-URA3-ade2-a</i>

nam7-Δ::natMX

Strains are derivatives of W303 with the common genotype *ade2-1 can1-100 his3-11,15 leu2-3,112 trp1-1 ura3-1 RAD5* except where noted.

Table S4. qPCR primers used in this study

Amplicon	Forward Primer	Reverse Primer
RAD55	AAGAGGCGGCGGAATGATAG	CGTTTGATTGGAAGGCGGTG
RAD57	GGATGGCAGAGAAGCTCCAA	CCAAGTAGCCACCCTAGCTG
RAD51	TTTGGGTGGTGGTGTGGAAA	CATGTCACGGCCAAAGTGTG
RAD52	ACTCGACGAAGAACCTGGTG	ACTGTTAGCCTCAGCAGGTG
RAD54	AGTGCTGTACGGTTGGATGG	TTGATACCACACCCACCTGC
CYH2 Intron*	CACTGTTGAGACGGCTTATTTGA	TTGCTCAGTTTGCGATGGAA
SCR1	GGCAAGGTAGTTCTGGGTCC	TCCATCACGGGTCACCTTTG